Pallidal Spectral and Phase-Amplitude Coupling Differences in Parkinson's Disease Locomotor States

Josephine J. Wallner[1*], Nicholas Druck[1*], Harsh P. Shah[2], Leslie J. Cloud[3,4], Kathryn L. Holloway[2], and Dean J. Krusienski[1]

[1]Biomedical Engineering, Virginia Commonwealth University
[2]Department of Neurosurgery, Virginia Commonwealth University Health System
[3]Parkinson's and Movement Disorders Center, Virginia Commonwealth University
[4]Department of Neurology, Virginia Commonwealth University Health System
[*]authors contributed equally

December 24, 2025

Corresponding author: Nicholas Druck. Department of Biomedical Engineering. 800 E Leigh St, Richmond, VA 23298, (804) 828-7929. Email: druckn@vcu.edu

Word count: 3697

Running title: GPi Spectra and PAC in PD Locomotor States

Financial Disclosure/COI: LC received grants in the past 3 years from MJFF, PF, and NIH, Trial Contracts (paid to university in past 3 years) from UCB, Cerevel, Amneal, Biogen, Bluerock, Intracellular Therapeutics and Bukwang. Advisory board for Amneal. Speakers bureau for Kyowa Kirin. 20% owner of Motion Medix, LLC.

Funding Sources: 2022 & 2024 Virginia Commonwealth University Parkinson's and Movement Disorders Center (PMDC) Pilot Grants. Virginia Commonwealth University Medical Scientist Training Program.

Abstract

Background: Deep brain stimulation of the subthalamic nucleus or Globus Pallidus internus is an established therapy for Parkinson's Disease that is sub-optimally managed with medication. While post-operative motor studies have defined neurophysiological signatures of the subthalamic nucleic local field potentials, comparable studies in the Globus pallidus internus are needed. Recent work shows that bandpower and phase-amplitude coupling in the subthalamic nucleus reliably distinguish locomotor states, motivating parallel investigation in the Globus pallidus internus.

Objectives: To characterize pallidal bandpower and phase-amplitude coupling across locomotor states (sitting, standing, and overground walking) in Parkinson's, and relate to clinical motor scores.

Methods: Bandpower and phase-amplitude coupling from pallidal signals of six adults with Parkinson's were compared across locomotor states; inter-state differences were correlated with clinical scores.

Results: High beta and gamma power differentiated sitting from walking, while delta power distinguished standing from walking. Phase-amplitude coupling between lower phases and gamma amplitude decreased during walking. Standing-to-walking delta-power modulation strongly correlated with Unified Parkinson's Disease Rating Scale scores ($R = 0.9$, $p < 0.05$). Standing-to-walking beta-gamma phase-amplitude coupling modulation highly correlated with freezing-of-gait scores ($R = 0.86$, $p < 0.05$).

Conclusions: This study provides the first detailed characterization of Globus pallidus internus activity in these locomotor states in Parkinson's. The coupling between lower frequencies and gamma was lower during walking as compared to sitting and standing, revealing an inverse relationship to what has been reported in the subthalmic nucleus. These findings suggest that movement coordination in the Globus pallidus internus may rely on a balance of single- and cross-frequency mechanisms.

1 Introduction

Parkinson's disease (PD) is a progressive neurodegenerative disorder marked by the loss of dopaminergic neurons in the substantia nigra (SN), leading to cardinal motor symptoms including rigidity, tremor, and bradykinesia [1]. The incidence of PD has been sharply rising; recent estimates from the Medicare administrative database suggest 90,000 new diagnoses for those 65 and older, representing a nearly 50% increase from a decade ago [2]. First-line treatment for motor symptoms in PD traditionally includes levodopa, an exogenous dopamine precursor that replenishes the diminished production in the SN [3]. While levodopa provides major improvements for many patients with PD, upwards of 85% may develop levodopa-induced dyskinesias or face a lack of clinical benefit following long-term administration [4]. Falling levels of plasma and cerebral levodopa hours after the initial dose increase a patient's susceptibility to experiencing "wearing-off" effects, which describe a gradual return of Parkinsonism (i.e., the benefit of levodopa disappears) [5]. The inconsistent responses and benefit from levodopa, among other PD medications, have prompted the implementation of therapeutic deep-brain stimulation (DBS) devices to achieve greater, long-term symptom relief. For PD that is sub-optimally managed with medication, DBS of the subthalamic nucleus (STN) or Globus Pallidus internus (GPi) has become standard practice. Aside from delivering electrical stimulation to these sites, modern DBS devices also enable intracranial recording of electrophysiological data in the form of local field potentials (LFPs) from the basal ganglia. This technology offers the opportunity to quantitatively link neural activity with observed motor behavior and symptom severity to optimize and fine-tune DBS delivery.

Current approaches to quantifying symptom severity and progression in PD largely rely on clinical rating scales and patient-reported outcomes [6]. The most widely used metric, the Unified Parkinson's Disease Rating Scale (UPDRS) motor subsection III, provides a structured clinical assessment of motor impairment [7, 8]. Similarly, the new Freezing of Gait Questionnaire (nFoG-Q) and related scales are employed to quantify the frequency and severity of freezing of gait (FoG), one of the most debilitating gait-related consequences of PD.

While these scales allow for the assessment of behavioral manifestations of PD, they do not directly reflect the underlying neural mechanisms that drive these symptoms. LFPs reflect the collective activity of neuronal populations proximal to a sensor. Extensive work in STN LFPs has identified electrophysiological markers of PD, such as excessive beta-band synchronization and beta-gamma phase-amplitude coupling (PAC) [9–12]. Of note, beta-gamma PAC has been extensively studied in

both non-invasive scalp electroencephalography (EEG), motor cortex electrocorticography, and invasive DBS STN neural data [11, 13, 14]. Beta-gamma PAC has been proposed to be a biomarker of PD and has been shown to be modulated by changes in gait patterns. [11, 13–17].

PAC has been implicated in inter-areal and local processes, with the former often interpreted as directed communication between neural regions [18]. Within regions, studies show that hippocampal PAC measures correlate with successful memory encoding and increase with working-memory load, while attention modulates PAC in visual cortex to improve discriminability [19, 20]. Local PAC changes within specific regions of the STN have shown to reliably differentiate between PD motor subtypes [21]. These findings suggest that local PAC could reflect a dynamic gating that regulates when neural populations become excitable or synchronized in response to task demands.

Studies of STN LFPs in PD during rest and movement revealed that splitting the beta band into sub-bands (ie., low beta: 13-20 Hz, high beta: 21-30 Hz) revealed distinct responses to stimulation and PAC dynamics with high frequency oscillation (HFO) [22–26]. This suggest beta sub-bands may represent separate processes in PD, albeit a similar investigation in the GPi remains lacking.

While the STN has been extensively characterized, the GPi remains comparatively less studied with respect to locomotion-related LFP dynamics. The GPi is the primary output nucleus of the basal ganglia, serving as the main integration center between subcortical and thalamo-corticol projections. Recent evidence suggests that the STN and pallidum play reciprocal, opposing roles with distinct oscillatory patterns observed across these structures [27–29]. Early GPi LFP studies in PD showed that low and high beta power and PAC with HFOs were differentially modulated by finger tapping and rest during intra-operative assessments [30]. To disentangle the contribution of pallidal neural signals during naturalistic behaviors such as standing and walking, it is necessary to record and analyze GPi LFPs outside of the operating room environment. Such analyses have the potential not only to further the understanding of GPi neurophysiology but also to develop new methods of quantifying markers of motor dysfunction, such as FoG.

While conventional DBS treatment delivers fixed-parameter continuous stimulation, the recent FDA approval of adaptive DBS (aDBS) allows for tailoring stimulation delivery based on LFP biomarkers. The implementation of aDBS may help ameliorate stimulation-induced side effects such as dyskinesias or FoG [31, 32]. In its current iteration, aDBS allows clinicians to modify stimulation parameters based on changes in pre-determined features. Such features, including STN-dervied excessive beta synchrony, have been identified through robust work during naturalistic locomotion and have shown great potential to serve as candidates for aDBS biomarkers. Nonetheless, an analogous biomarker for GPi aDBS remains largely lacking, and would enhance the clinician's ability to optimize DBS treatments across PD-relevant DBS targets.

The current study provides a spectral characterization of GPi LFPs during sitting, standing, and overground walking. These results demonstrate the feasibility of capturing locomotor-state-related neurodynamics in the GPi and provide a framework for future studies probing FoG mechanisms and refining aDBS strategies.

2 Methods

2.1 Participants and DBS devices

Six participants diagnosed with PD were recruited for the study. All participants reported persistent FoG following DBS implantation. The study design was approved by the Institutional Review Board of Virginia Commonwealth University, and informed consent was obtained for experimentation with human subjects. All participants were implanted with the Percept (Medtronic, Minneapolis, MN) DBS system in the GPi (unilateral or bilateral, based on clinical indication - see table in Figure S1) [33]. Each electrode shaft consists of four contacts, forming three bipolar recording channels (i.e., C0-C2, C1-C3, C0-C3). The Percept system records LFPs digitized at 250 Hz. All data were recorded using the Percept's Indefinite Streaming mode, which is done with stimulation off. Patient demographics, clinical characteristics, and device setup can be found in Figure S1.

2.2 Data Collection

The participants walked an obstacle course that was originally designed to elicit FoG. Minimal freezing data were obtained during the experimental sessions, and excluded from the subsequent analysis. The course consisted of five scenarios while LFPs were recorded: (1) passing a narrow archway, (2) 540° turn, (3) approaching a visual target, (4) dual-task (performing calculations while walking), and (5) a time-sensitive task (answering a distant ringing phone). Data were collected off medication and with stimulation off. A summary of data length across participants is listed in Table 1.

Condition \ Participant	A	B	C	D	E	F
Sit	120	127	10	38	60	102
Stand	120	12	120	30	51	20
Walk	120	130	130	120	98	120

Table 1: Seconds of data collected in each locomotor state across participants A–F.

During the experimental sessions, participants donned ankle-mounted inertial monitoring units (IMUs), which were temporally aligned with GPi LFP recordings through the injection of a controlled external artifact. Transcutaneous electrical nerve stimulation (TENS) electrodes were positioned on the lateral neck, over the subcutaneous DBS leads, and on the contralateral mastoid. Surface EMG electrodes placed adjacent to the DBS leads detected the TENS artifact. Both EMG and IMU data streams were routed to a laptop via Lab Streaming Layer (LSL) for synchronized acquisition [34]. The TENS artifact, present in both the IMU and LFP signals, enabled offline temporal alignment.

Video recordings were acquired concurrently and synchronized to IMU and LFP data using timestamps and audio markers. Additionally, an external audio signal was transmitted through LSL to serve as a secondary synchronization marker across the video and IMU recordings. Based on the synchronized IMU and video data, the LFP recordings were manually segmented into three locomotor states: sitting, standing, and walking.

2.3 Data Analysis

2.3.1 Preprocessing

To provide a balanced comparison across participants with differing number of implants, a single hemisphere was chosen for analysis. For those with bilateral implants, GPi contacts contralateral to hemibody with worse (ie., greater) UPDRS-III scores at the time of collection were chosen. One participant had equal UPDRS-III scores bilaterally; for this participant, the initially affected hemisphere per prior clinical documentation was used. For all participants, the C1 and C2 contacts were confirmed to be located in the GPi by a neurosurgeon via post-operative imaging using Stealth MRI (Medtronic, Minneapolis, MN) [33]. From these contacts, two bipolar channels based on the C0-C2 and C1-C3 contact pairs were used for the subsequent analyses. Channel C0-C3 was not analyzed due to the lower spatial specificity and overlap with the selected channels. The raw LFP data and power spectra were screened to confirm the absence of motion artifacts, and for EKG contamination using the Perceive toolbox [35]. Dual-tasking walking data was excluded to avoid confounding effects in the signals. While some participants had shorter lengths of clean LFPs, the subsequent analysis techniques have been shown to be robust for these segment lengths [36].

2.3.2 Frequency Bandpower

Bandpower estimates were calculated to quantify the relative contributions of physiological frequencies across locomotor states. The power spectral densities (PSDs) were estimated for each locomotor state using Welch's method via the *pwelch* function in MATLAB2024a (MathWorks Inc., Natick, MA). The LFPs were partitioned into 1-second Hamming-windowed epochs with 50% overlap. Due to the lowpass filter characteristics of the Percept, the resulting PSDs were processed and visualized up to 100 Hz.

To reveal differences in bandpower between locomotor states, the *bandpower* function in MATLAB2024a was used across canonical frequency bands (i.e., Delta: 0.5-4 Hz, Theta: 4-8 Hz, Alpha:

8-12 Hz, Beta: 13-30 Hz, and Gamma: 30-100 Hz). Based on prior work suggesting functionally relevant subdivisions of the beta band in the GPi, low beta (13-20 Hz) and high beta (21-30 Hz) were also analyzed [30].

Pairwise statistical comparisons between locomotor states were performed separately for each frequency band using the Wilcoxon signed-rank test, a nonparametric test that does not assume normality. P-values were adjusted for multiple comparisons using Benajmini-Hochberg correction (significance threshold: 0.05).

2.3.3 Phase-Amplitude Coupling

Phase-amplitude coupling (PAC) was quantified using the modulation index (MI) based on Kullback–Leibler divergence, a widely-used method in LFP studies [23, 30, 36]. LFP signals were bandpass filtered to estimate phase frequencies from 1–30 Hz (1 Hz steps, 2 Hz bandwidth) and amplitude frequencies from 40–100 Hz (2 Hz steps, 10 Hz bandwidth). Instantaneous phase and amplitude were extracted using the Hilbert transform. Specifically, for every 20-degree interval of the instantaneous phase distribution, the entropy of the instantaneous amplitude envelope distribution was computed.

MI values were computed between each phase–amplitude frequency pair and visualized as comodulograms. To obtain summary PAC metrics, MI values were summed across canonical phase-frequency ranges, consistent with prior DBS work. [11]:

$$\text{PAC} = \sum_{\text{phase range}} MI \tag{1}$$

where *phase range* represents the minimum and maximum phase frequencies used for the summation of MI values. This process was repeated for each locomotor state.

Pairwise statistical comparisons between locomotor states were performed using Wilcoxon signed-rank tests with Benjamini–Hochberg correction (significance threshold: 0.05).

2.3.4 Clinical Correlations

The resulting bandpower and PAC comparisons that yielded statistically significant differences were linearly correlated to the clinical motor scores (UPDRS-III, nFoG-Q) using robust linear regression. Specifically, the difference between each significant bandpower or PAC combination was calculated for all GPi contacts and averaged within each participant.

3 Data Sharing

Data are available upon request.

4 Results

4.1 Differences in frequency bandpower across locomotor states

Figure 1a shows average PSDs across all participants for all three locomotor states: sit, stand, and walk. The power in specific frequency bands was averaged for each participant and each state, and displayed as box plots in Figure 1b. Individual PSDs for all GPi contacts can be found in Figure S2.

Pairwise comparisons between locomotor states revealed increased delta power during walking relative to standing. Power in both high beta and gamma frequency ranges differentiated between sitting and walking: walking was associated with decreased high beta and increased gamma. Notably, the beta power modulation between sitting and walking was not apparent when analyzing the entire beta range as a single band.

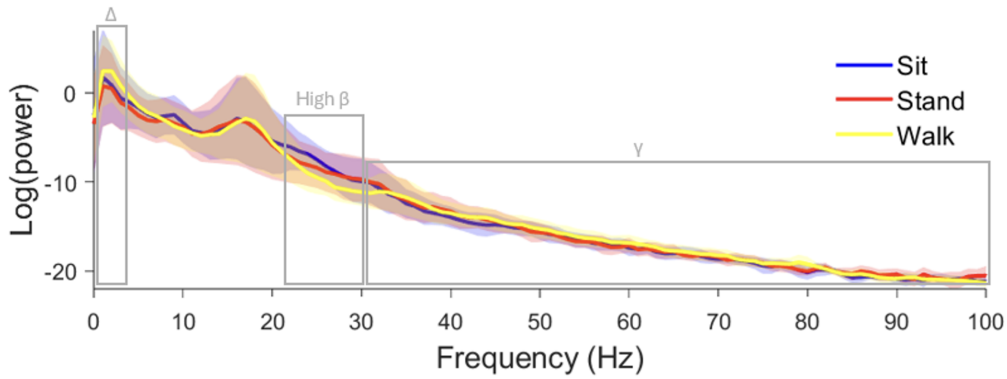

(a) Power spectral densities for each locomotor state, averaged across participants. Solid lines indicate mean, with shaded regions indicating 95% confidence intervals. The boundaries of the frequency ranges exhibiting significant differences between states are highlighted with gray boxes.

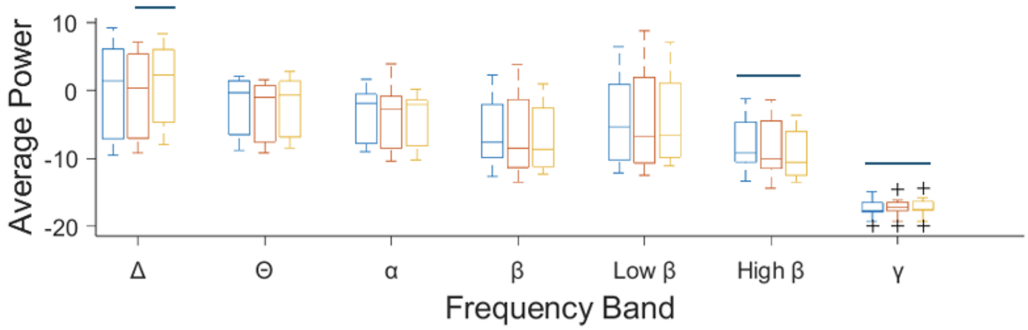

(b) Box plots of the bandpower distributions across participants for each frequency band. Horizontal bars indicate statistically significant differences ($p < 0.05$)

.

Figure 1: Summary of bandpower analysis across locomotor states.

4.2 Differences in phase-amplitude coupling across locomotor states

Figure 2a provides example comodulograms for one contact from one participant across locomotor states. The insets highlight the coupling between the phase of canonical frequency ranges (i.e., theta, alpha, beta) and the gamma amplitude. PAC values from these comodulograms were summarized into locomotor-state-specific boxplots, as shown in Figure 2b. Individual comodulograms for GPi contacts across all participants can be found in Figure S3.

No significant differences in PAC were observed between sitting and standing. However, compared to sitting and standing, walking was consistently associated with a decrease in PAC between all lower frequency bands and gamma. Standing-related PAC is highest at low phase frequencies and gradually declines with increasing phase frequency, similar to the typical 1/f-like decay in neural power spectra; however, these PAC patterns cannot be fully accounted for by frequency-dependent changes in power [37]. This difference across locomotor states was present whether or not the beta band was partitioned into low and high beta; therefore, subsequent PAC comparisons were done so using the entire beta band without sub-divisions.

Figure 3 compares the current GPi beta–gamma PAC results with previously published STN findings from Farokhniaee et al. (2024) [11]. To enable an analogous comparison, the beta–gamma PAC values from Figure 2b were min–max normalized to match the scale in the STN analysis. In this STN study, beta-gamma PAC was positively modulated during walking across their participants; whereas in this GPi cohort, a reciprocal trend was observed where beta-gamma PAC was negatively modulated during walking.

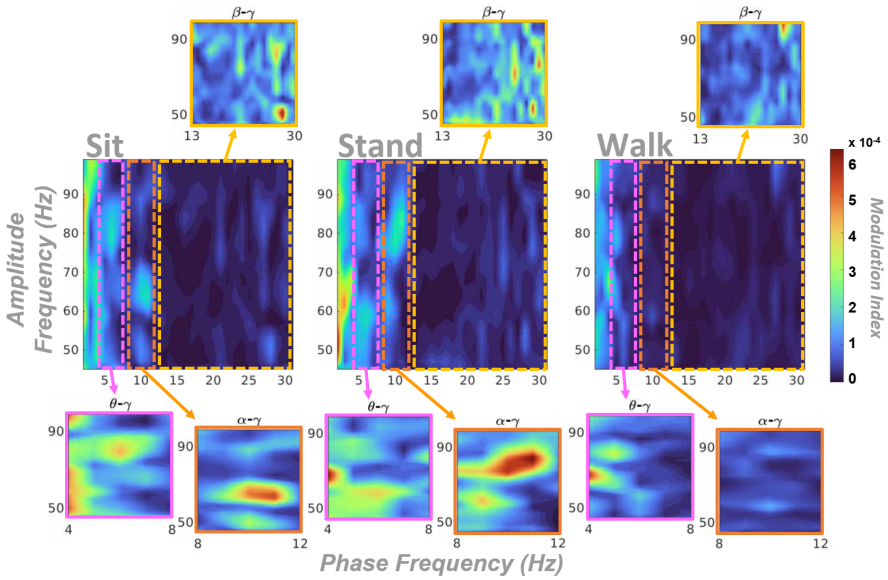

(a) Locomotor state-specific comodulograms for one contact from an example participant. The larger three comodulograms labeled "Sit", "Stand", and "Walk", share the displayed color scale. MI values across locomotor states, and within a phase frequency range inset, were re-normalized to better visualize coupling dynamics that are otherwise obscured by the shared color scale. State- and phase range-specific PAC values were estimated, using Eq. 1.

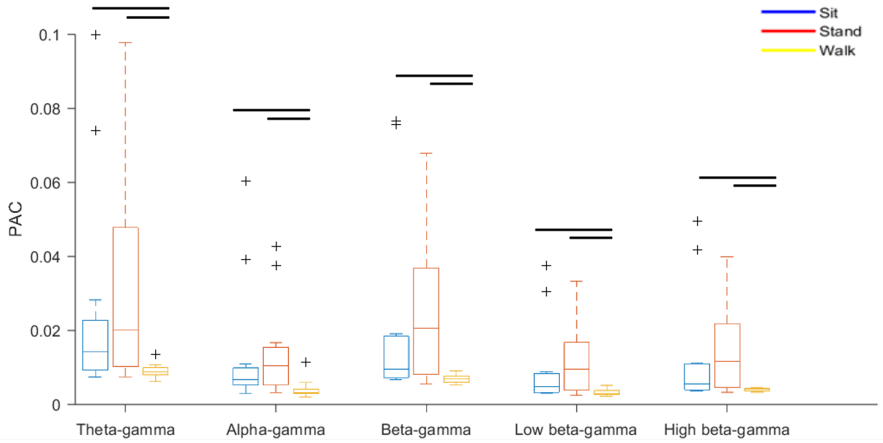

(b) Box plots of the PAC values for all participants and for each frequency band pair. Horizontal bars indicate statistically significant differences ($p < 0.05$, with Benjamini-Hochberg correction).

Figure 2: Summary of the PAC analysis across locomotor states.

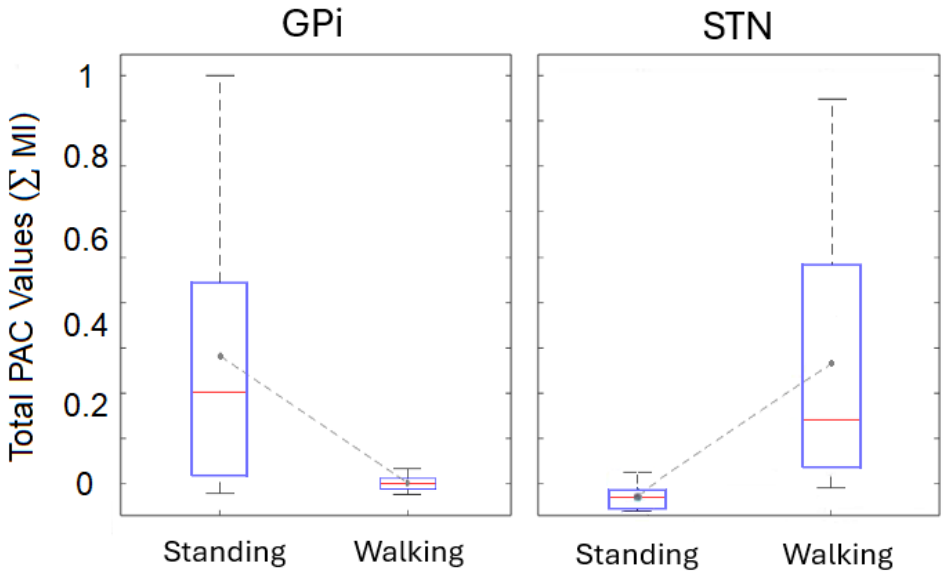

Figure 3: Min-max normalized changes in beta-gamma PAC between standing and walking, compared between the present GPi participants and a separate STN cohort from Farokhniaee et al., 2024 [11]. Beta-gamma PAC between standing and walking exhibits a reciprocal relationship across STN and GPi.

4.3 Correlations between spectral features and clinical motor scores

Statistically significant spectral features (i.e., delta power modulation and beta–gamma PAC differences) were averaged across each participant's GPi contacts to yield a single representative value per participant. These spectral features were then correlated with clinical motor scores using MATLAB's built-in *fitlm* function with the *RobustOpt* parameter set to *on*. Results of robust regression correlations across all spectral features can be found in Figure S5.

In Figure 4a, the correlation between standing-to-walking delta modulation with UPDRS-III scores is shown. In Figure 4b, the correlations between standing-to-walking beta-gamma PAC modulation and clinical motor scores is shown.

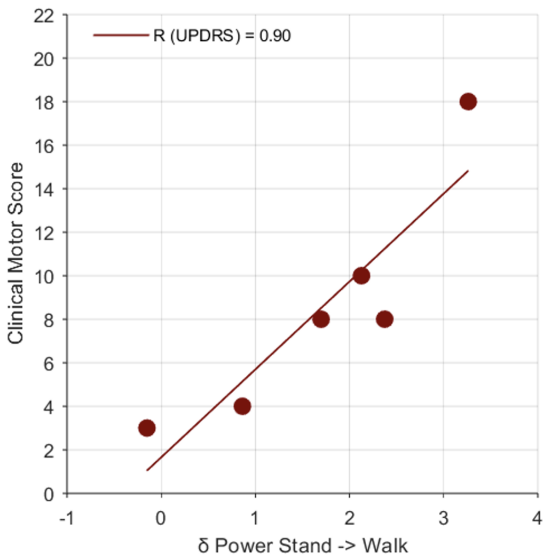

(a) Robust linear regression between delta power modulation from standing to walking with UPDRS scores. Individual points represent the averaged delta modulation for each participant (p_{fog} = 0.01).

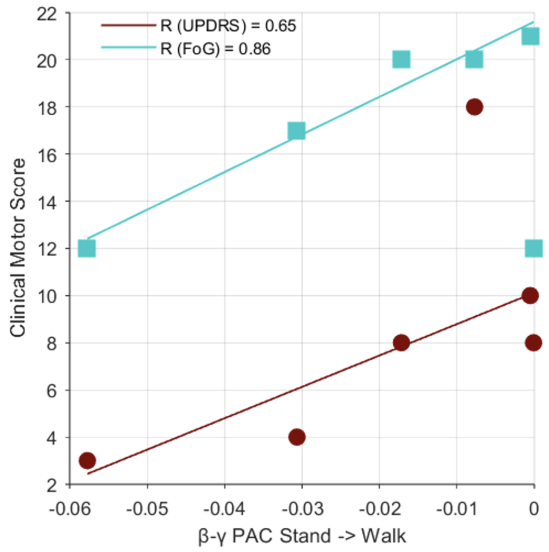

(b) Robust linear regression between the beta-gamma PAC modulation from standing to walking with both UPDRS-III and nFoG-Q scores. Individual points represent the averaged beta-gamma PAC modulation from standing to walking for each participant (p_{updrs} = 0.18, p_{fog} = 0.04).

Figure 4: Robust linear correlations between selected statistically-significant spectral and PAC features and clinical motor scores.

5 Discussion

This study examined single-frequency and cross-frequency pallidal dynamics during naturalistic locomotor states in PD and their relationship to clinical motor scores. High beta and gamma power differentiated sitting from walking, while delta power distinguished standing from walking. PAC between all lower phases and gamma amplitude decreased during walking. Delta-power modulation between standing and walking strongly correlated with UPDRS motor scores. Beta-gamma PAC modulation highly correlated with nFOG-Q.

When analyzing bandpower, dividing beta into low- and high-frequency sub-bands revealed interstate differences that were obscured when beta was treated as a single range, suggesting that distinct beta components modulate differentially to locomotor control. Beta suppression during movement is consistent with well-established evidence that movement-related beta desynchronization underlies healthy motor output and is disrupted in PD [38–40]. The accompanying gamma and delta modulation during walking suggests that multiple oscillations reconfigure as participants transition between static and dynamic locomotor states, underscoring the distributed, multi-frequency nature of motor control. Of note, the observed positive modulation in delta power from standing to walking aligns with prior work that simultaneously recorded from the GPi and pedunculopontine nucleus (PPN), an upper brainstem region with strong reciprocal connections to the basal ganglia [41]. This study reported increased activity in the 1-8 Hz range during walking, suggesting that low-frequency oscillations may be a shared signature of gait-related state transitions across interconnected nodes of the motor network. When considered alongside the present findings, this raises the possibility that GPi LFPs partly reflect upstream state-dependent inputs from the PPN or related locomotor regions, rather than solely local pallidal processes. However, the present dataset cannot distinguish afferent versus intrinsic sources of these low-frequency changes and the aforementioned study did not report the same low frequency modulation in the GPi during walking. Hence, this interpretation should be tentatively viewed as a mechanistic hypothesis for future testing.

PAC between lower-frequency phases (theta, alpha, and beta) and gamma amplitude were found to be globally reduced during walking (Fig. 2b). In line with previous work suggesting a role for local

PAC in dynamic gating, this reduction could reflect the lowering of an inhibitory signal from the GPi during active movement. Importantly, the consistent pattern of stand $\approx$ sit $>$ walk across all lower-frequency phase-gamma amplitude interactions suggests that PAC in the GPi may encode a global movement-related control signal rather than a frequency-specific process. Similar across-frequency band movement-related changes in spectral measures have been reported in PD. A previous scalp EEG study in PD participants with FoG observed that during both locomotion- and non-locomotion-based tasks, inter- and intra-hemispheric connectivity was significantly increased relative to healthy controls, agnostic of the frequency band [42]. This overall increase in connectivity, analogously observed in other neurodegenerative diseases such as Alzheimer's Disease, has been suggested to serve as a protective compensatory response to the process of neurodegeneration [43].

Work in the STN has reported that beta-gamma PAC was positively modulated during walking relative to standing, an opposing finding to the observed GPi trend shown in Figure 3. This discrepancy may underlie the reciprocal movement-related neurophysiological roles of the STN and GPi in the basal ganglia circuit [11, 27, 44].

When incorporating clinical data, delta modulation between standing and walking correlated with UPDRS-III motor scores (Fig. 4a), while beta–gamma PAC modulation correlated with nFoG-Q scores (Fig. 4b). Participants with higher UPDRS-III scores exhibited larger standing-to-walking delta shifts, suggesting that low-frequency dynamics may become dysregulated as motor symptoms worsen. Conversely, reduced modulation of beta-gamma coupling tracked the severity of motor symptoms, as reflected in nFoG-Q scores. Reduced beta–gamma modulation may indicate a loss of flexible cross-frequency coordination in basal ganglia circuits, limiting the system's ability to transition between static and active locomotor states as motor symptoms worsen. Interestingly, beta and gamma power modulation do not correlate to clinical motor scores in the same way, suggesting that in these higher frequencies, the motor pathologies may reflect more as an impairment in cross-frequency coupling, as opposed to simple power modulations seen in lower frequencies, such as delta. Beyond the well-known elevation of band-specific oscillatory power in PD, the observed reduction in PAC modulation points to diminished flexibility in cross-frequency communication, which may underlie impaired motor adaptability.

This study has several limitations. First, the sample size was relatively small, which may limit the generalizability of the findings and reduce statistical power to detect differences in the GPi across locomotor states. In particular, this small sample size poses a challenge for interpreting the clinical correlations presented in this study. While it is vital to connect spectral features to existing clinical scales, larger cohorts are necessary to support this association. Second, participants displayed variable disease duration (table in Figure S1) and medication regimens, which could have influenced basal ganglia activity. This, combined with the slow dissipation of stimulation effects in the GPi, likely contributed to variability in the GPi measures across tasks [45]. Finally, while the MI is widely used to quantify PAC, it can be sensitive to noise, filtering choices, and non-sinusoidal waveforms. MI, like other measures of cross-frequency coupling, captures statistical associations but does not reveal the underlying mechanism, and may reflect common neural sources rather than true physiological interactions. These factors may limit the interpretability of PAC results in assessing pallidal activity across locomotor states in PD.

These results carry clear implications for aDBS. Incorporating multi-band, state-aware biomarkers such as delta modulation or beta–gamma PAC may enhance adaptive control by accounting for locomotor context. Longitudinal tracking of these markers' modulation could also provide a physiological tracker of disease progression as well as neural state fluctuations on a shorter timescale, guiding parameter adjustments over time.

6 Acknowledgments

This work was funded in part by 2022 & 2024 Virginia Commonwealth University Parkinson's and Movement Disorders Center (PMDC) Pilot Grants. The authors would also like to thank Gina Marie Blackwell for her assistance in obtaining the IRB approval, and patient coordination and in addition, Alex Feria for data collection. Additionally, the authors are grateful to Ken Koltermann and Gang Zhou for providing the ankle inertial measurement units and their associated synchronization software.

7 Authors' Roles

Conceptualization and study design: JW, HS, LC, KH, DJK; Data collection: JW, ND, HS, LC, KH; Formal analysis: JW, ND; Manuscript preparation: JW, ND, DJK; Manuscript review & editing: JW, ND, HS, LC, KH, DJK

8 Financial Disclosures

JW, ND, DJK, HS, KH: None; LC: Grants (in past 3 years) from MJFF, PF, and NIH Trial Contracts (paid to university in past 3 years) from UCB, Cerevel, Amneal, Biogen, Bluerock, Intracellular Therapeutics and Bukwang Advisory board for Amneal. Speakers bureau for Kyowa Kirin. 20% owner of Motion Medix, LLC.

References

[1] Saman Zafar and Sridhara S Yaddanapudi. Parkinson disease. In *StatPearls*. StatPearls Publishing, Treasure Island (FL), January 2025.

[2] A W Willis, E Roberts, J C Beck, B Fiske, W Ross, R Savica, S K Van Den Eeden, C M Tanner, C Marras, and Parkinson's Foundation P4 Group. Incidence of parkinson disease in north america. *NPJ Parkinsons Dis.*, 8(1):170, December 2022.

[3] Kavita R Gandhi and Abdolreza Saadabadi. Levodopa (l-dopa). In *StatPearls*. StatPearls Publishing, Treasure Island (FL), January 2025.

[4] Milan Beckers, Bastiaan R Bloem, and Marcel M Verbeek. Mechanisms of peripheral levodopa resistance in parkinson's disease. *NPJ Parkinsons Dis.*, 8(1):56, May 2022.

[5] Joseph Jankovic, Mark Hallett, Michael S. Okun, Cynthia Comella, Stanley Fahn, and Jennifer Goldman. Chapter 6 - medical treatment of the motor features of parkinson disease. In Joseph Jankovic, Mark Hallett, Michael S. Okun, Cynthia Comella, Stanley Fahn, and Jennifer Goldman, editors, *Principles and Practice of Movement Disorders (Third Edition)*, pages 164–203.e14. Elsevier, London, third edition edition, 2021.

[6] Ghayth AlMahadin, Ahmad Lotfi, Eva Zysk, Francesco Luke Siena, Marie Mc Carthy, and Philip Breedon. Parkinson's disease: current assessment methods and wearable devices for evaluation of movement disorder motor symptoms - a patient and healthcare professional perspective. *BMC Neurol.*, 20(1):419, November 2020.

[7] Movement Disorder Society Task Force on Rating Scales for Parkinson's Disease. The unified parkinson's disease rating scale (UPDRS): status and recommendations. *Mov. Disord.*, 18(7):738–750, July 2003.

[8] Alice Nieuwboer, Lynn Rochester, Talia Herman, Wim Vandenberghe, GE Emil, T Thomaes, and Nir Giladi. Reliability of the new freezing of gait questionnaire: Agreement between patients with Parkinson's disease and their carers. *Gait & Posture*, 30:459–463, 2009.

[9] Thomas Koeglsperger, Jan H Mehrkens, and Kai Bötzel. Bilateral double beta peaks in a PD patient with STN electrodes. *Acta Neurochir. (Wien)*, 163(1):205–209, January 2021.

[10] Natasha Darcy, Roxanne Lofredi, Bassam Al-Fatly, Wolf-Julian Neumann, Julius Hübl, Christof Brücke, Patricia Krause, Gerd-Helge Schneider, and Andrea Kühn. Spectral and spatial distribution of subthalamic beta peak activity in parkinson's disease patients. *Exp. Neurol.*, 356(114150):114150, October 2022.

[11] Amirali Farokhniaee, Chiara Palmisano, Jasmin Del Vecchio Del Vecchio, Gianni Pezzoli, Jens Volkmann, and Ioannis U Isaias. Gait-related beta-gamma phase amplitude coupling in the subthalamic nucleus of parkinsonian patients. *Sci. Rep.*, 14(1):6674, March 2024.

[12] Andrew I Yang, Nora Vanegas, Codrin Lungu, and Kareem A Zaghloul. Beta-coupled high-frequency activity and beta-locked neuronal spiking in the subthalamic nucleus of parkinson's disease. *J. Neurosci.*, 34(38):12816–12827, September 2014.

[13] Yuki Kimoto, Naoki Tani, Takuto Emura, Takahiro Matsuhashi, Takuto Yamamoto, Yuya Fujita, Satoru Oshino, Koichi Hosomi, Hui Ming Khoo, Shimpei Miura, Takahiro Fujinaga, Takufumi Yanagisawa, and Haruhiko Kishima. Beta-gamma phase-amplitude coupling of scalp electroencephalography during walking preparation in parkinson's disease differs depending on the freezing of gait. *Front. Hum. Neurosci.*, 18:1495272, November 2024.

[14] Zhen Yin, Guoping Zhu, Yuchen Liu, Bin Zhao, Dandan Liu, Yiqing Bai, Qiqi Zhang, Lei Shi, Tao Feng, Aiping Yang, Hongli Liu, Fangang Meng, Wolfgang J Neumann, Andrea A Kühn, Yuan Jiang, and Jianfeng Zhang. Cortical phase-amplitude coupling is key to the occurrence and treatment of freezing of gait. *Brain*, 145(7):2407–2421, 2022.

[15] Tisa Hodnik, Stiven Roytman, Nico I Bohnen, and Uros Marusic. Beta-gamma phase-amplitude coupling as a non-invasive biomarker for parkinson's disease: Insights from electroencephalography studies. *Life (Basel)*, 14(3):391, March 2024.

[16] Haifeng Zhao, Shenglin Hao, Peiran Zhang, Shenghong He, Laura Wehmeyer, Ziyi Feng, Lu Xu, Shikun Zhan, Wei Liu, Xiaoxiao Zhang, Marie-Laure Welter, Dianyou Li, Bomin Sun, Yong Lu, Huiling Tan, and Chunyan Cao. Cortical and corticomuscular beta-gamma phase-amplitude coupling during different locomotion states and the effects of levodopa in parkinson's disease. *Mov. Disord.*, (mds.70031), September 2025.

[17] Philipp A. Loehrer, Sahar Yassine, Immo Weber, Valentin Sanner, Shenghong He, Alek Pogosyan, Lijiao Chen, Laura Witt, Gereon Rudolf Fink, David J. Pedrosa, Lars Timmermann, and Huiling Tan. Characterizing the frequency-specific and spatiotemporal dynamics of - phase-amplitude coupling in parkinson's disease. *bioRxiv*, 2025.

[18] Xian Jiang, Jorge Gonzalez-Martinez, and Eric Halgren. Inter-area theta-gamma phase–amplitude coupling supports directed communication in the primate brain. *Scientific Reports*, 9:13487, 2019.

[19] Bradley Lega, John Burke, Joshua Jacobs, and Michael Kahana. Slow-theta-to-gamma phase–amplitude coupling in human hippocampus supports the formation of new episodic memories. *Cerebral Cortex*, 26(1):268–278, 2016.

[20] Aniruddh S. Nandy, Jonathan J. Nassi, and John H. Reynolds. Attention decreases phase–amplitude coupling, enhancing stimulus discriminability in cortical area mt. *Frontiers in Neural Circuits*, 9:82, 2016.

[21] Ilknur Telkes, Ashwin Viswanathan, Joohi Jimenez-Shahed, Aviva Abosch, Musa Ozturk, Akshay Gupte, Joseph Jankovic, and Nuri F Ince. Local field potentials of subthalamic nucleus contain electrophysiological footprints of motor subtypes of parkinson's disease. *Proceedings of the National Academy of Sciences*, 115(36):E8567–E8576, 2018.

[22] Joohi Jimenez-Shahed, Ilknur Telkes, Ashwin Viswanathan, and Nuri F Ince. GPi oscillatory activity differentiates tics from the resting state, voluntary movements, and the unmedicated parkinsonian state. *Front. Neurosci.*, 10:436, September 2016.

[23] Jon López-Azcárate, Mikel Tainta, María C Rodríguez-Oroz, Miguel Valencia, Rafael González, Jorge Guridi, Jorge Iriarte, José A Obeso, Julio Artieda, and Manuel Alegre. Coupling between beta and high-frequency activity in the human subthalamic nucleus may be a pathophysiological mechanism in parkinson's disease. *J. Neurosci.*, 30(19):6667–6677, May 2010.

[24] Bernadette C M van Wijk, Martijn Beudel, Ashwani Jha, Ashwini Oswal, Tom Foltynie, Marwan I Hariz, Patricia Limousin, Ludvic Zrinzo, Tipu Z Aziz, Alexander L Green, Peter Brown, and Vladimir Litvak. Subthalamic nucleus phase-amplitude coupling correlates with motor impairment in parkinson's disease. *Clin. Neurophysiol.*, 127(4):2010–2019, April 2016.

[25] Ashwini Oswal, Martijn Beudel, Ludvic Zrinzo, Patricia Limousin, Marwan Hariz, Tom Foltynie, Vladimir Litvak, and Peter Brown. Deep brain stimulation modulates synchrony within spatially and spectrally distinct resting state networks in parkinson's disease. *Brain*, 139(5):1482–1496, 03 2016.

[26] Musa Ozturk, Aviva Abosch, David Francis, Jianping Wu, Joohi Jimenez-Shahed, and Nuri F Ince. Distinct subthalamic coupling in the on state describes motor performance in parkinson's disease. *Movement Disorders*, 35(1):91–100, 2020.

[27] Christoph Wiest, Flavie Torrecillos, Alek Pogosyan, Manuel Bange, Muthuraman Muthuraman, Sergiu Groppa, Natasha Hulse, Harutomo Hasegawa, Keyoumars Ashkan, Fahd Baig, Francesca Morgante, Erlick A Pereira, Nicolas Mallet, Peter J Magill, Peter Brown, Andrew Sharott, and Huiling Tan. The aperiodic exponent of subthalamic field potentials reflects excitation/inhibition balance in parkinsonism. *eLife*, 12:e82467, feb 2023.

[28] Kara A Johnson, Jackson N Cagle, Janine Lobo Lopes, Joshua K Wong, Michael S Okun, Aysegul Gunduz, Aparna Wagle Shukla, Justin D Hilliard, Kelly D Foote, and Coralie de Hemptinne. Globus pallidus internus deep brain stimulation evokes resonant neural activity in parkinson's disease. *Brain Communications*, 5(2):fcad025, 02 2023.

[29] Stephen L. Schmidt, David T. Brocker, Brandon D. Swan, Dennis A. Turner, and Warren M. Grill. Evoked potentials reveal neural circuits engaged by human deep brain stimulation. *Brain Stimulation*, 13(6):1706–1718, 2020.

[30] Nicholas AuYong, Mahsa Malekmohammadi, Joni Ricks-Oddie, and Nader Pouratian. Movement-modulation of local power and phase amplitude coupling in bilateral globus pallidus interna in parkinson disease. *Front. Hum. Neurosci.*, 12:270, July 2018.

[31] Simon Little, Alex Pogosyan, Spencer Neal, Baltazar Zavala, Ludvic Zrinzo, Marwan Hariz, Thomas Foltynie, Patricia Limousin, Keyoumars Ashkan, James FitzGerald, Alexander L Green, Tipu Z Aziz, and Peter Brown. Adaptive deep brain stimulation in advanced parkinson disease. *Ann. Neurol.*, 74(3):449–457, September 2013.

[32] Kevin B Wilkins, Matthew N Petrucci, Emilia F Lambert, Jillian A Melbourne, Aryaman S Gala, Pranav Akella, Laura Parisi, Chuyi Cui, Yasmine M Kehnemouyi, Shannon L Hoffman, Sudeep Aditham, Cameron Diep, Hannah J Dorris, Jordan E Parker, Jeffrey A Herron, and Helen M Bronte-Stewart. Beta burst-driven adaptive deep brain stimulation for gait impairment and freezing of gait in parkinson's disease. *Brain Commun.*, 7(4):fcaf266, July 2025.

[33] Medtronic, Inc. Percept PC deep brain stimulator, 2020. https://www.medtronic.com.

[34] Lsl-website. https://labstreaminglayer.org/#/. Accessed: 2025-11-14.

[35] neuromodulation. perceive: MATLAB toolbox for extracting data from the medtronic percept bidirectional brain–computer interface. https://github.com/neuromodulation/perceive, 2020. Accessed: 2025-11-14.

[36] Adriano B L Tort, Robert Komorowski, Howard Eichenbaum, and Nancy Kopell. Measuring phase-amplitude coupling between neuronal oscillations of different frequencies. *J. Neurophysiol.*, 104(2):1195–1210, August 2010.

[37] Charmaine Demanuele, Christopher J James, and Edmund Js Sonuga-Barke. Distinguishing low frequency oscillations within the 1/f spectral behaviour of electromagnetic brain signals. *Behav. Brain Funct.*, 3(1):62, December 2007.

[38] Clara Moisello, Daniella Blanco, Jing Lin, Priya Panday, Simon P Kelly, Angelo Quartarone, Alessandro Di Rocco, Chiara Cirelli, Giulio Tononi, and M Felice Ghilardi. Practice changes beta power at rest and its modulation during movement in healthy subjects but not in patients with parkinson's disease. *Brain Behav.*, 5(10):e00374, October 2015.

[39] Varvara Mathiopoulou, Roxanne Lofredi, Lucia K Feldmann, Jeroen Habets, Natasha Darcy, Wolf-Julian Neumann, Katharina Faust, Gerd-Helge Schneider, and Andrea A Kühn. Modulation of subthalamic beta oscillations by movement, dopamine, and deep brain stimulation in parkinson's disease. *NPJ Parkinsons Dis.*, 10(1):77, April 2024.

[40] Elizabeth Heinrichs-Graham, Tony W Wilson, Pamela M Santamaria, Sheila K Heithoff, Diego Torres-Russotto, Jessica A L Hutter-Saunders, Katherine A Estes, Jane L Meza, R L Mosley, and Howard E Gendelman. Neuromagnetic evidence of abnormal movement-related beta desynchronization in parkinson's disease. *Cereb. Cortex*, 24(10):2669–2678, October 2014.

[41] Rene Molina, Chris J Hass, Kristen Sowalsky, Abigail C Schmitt, Enrico Opri, Jaime A Roper, Daniel Martinez-Ramirez, Christopher W Hess, Kelly D Foote, Michael S Okun, and Aysegul Gunduz. Neurophysiological correlates of gait in the human basal ganglia and the PPN region in parkinson's disease. *Front. Hum. Neurosci.*, 14:194, June 2020.

[42] Eitan E Asher, Meir Plotnik, Moritz Günther, Shay Moshel, Orr Levy, Shlomo Havlin, Jan W Kantelhardt, and Ronny P Bartsch. Connectivity of EEG synchronization networks increases for parkinson's disease patients with freezing of gait. *Commun. Biol.*, 4(1):1017, August 2021.

[43] William J Jagust and Elizabeth C Mormino. Lifespan brain activity, β-amyloid, and alzheimer's disease. *Trends Cogn. Sci.*, 15(11):520–526, November 2011.

[44] Atsushi Nambu, Hironobu Tokuno, and Masahiko Takada. Functional significance of the cortico–subthalamo–pallidal 'hyperdirect' pathway. *Neuroscience Research*, 43(2):111–117, 2002.

[45] Scott E Cooper, Cameron C McIntyre, Hubert H Fernandez, and Jerrold L Vitek. Association of deep brain stimulation washout effects with parkinson disease duration. *JAMA Neurol.*, 70(1):95–99, January 2013.